

Non-zero tensor condensates in cold quark matter within the three-flavor Nambu-Jona-Lasinio model with the Kobayashi-Maskawa-'t Hooft interaction

Ai KAGAWA¹, Masatoshi MORIMOTO¹, Yasuhiko TSUE^{2,3}, João da PROVIDÊNCIA³,
Constança PROVIDÊNCIA³ and Masatoshi YAMAMURA^{3,4}

¹*Graduate School of Integrated Arts and Science, Kochi University, Kochi 780-8520, Japan*

²*Department of Mathematics and Physics, Kochi University, Kochi 780-8520, Japan*

³*CFisUC, Departamento de Física, Universidade de Coimbra, 3004-516 Coimbra, Portugal*

⁴*Department of Pure and Applied Physics, Faculty of Engineering Science, Kansai University, Suita 564-8680, Japan*

The possible formation of tensor condensates originated from a tensor-type interaction between quarks is investigated in the three-flavor Nambu-Jona-Lasinio model including the Kobayashi-Maskawa-'t Hooft interaction, which leads to flavor mixing. It is shown that independent two tensor condensates appear and a tensor condensate related to the strange quark easily occurs by the effect of the flavor mixing compared with one related to light quarks. Also, it is shown that the tensor condensate related to the strange quark appears at a slightly smaller chemical potential if the Kobayashi-Maskawa-'t Hooft interaction is included, due to the flavor mixing effect. It is also shown that the two kinds of tensor condensates may coexist in a certain quark chemical potential due to the flavor mixing.

§1. Introduction

One of recent interests in many-quark system governed by quantum chromodynamics (QCD) is to clarify the existence of various phases on the plane spanned by the quark chemical potential and temperature.¹⁾ As is indicated by many authors, there may exist various phases such as the color superconducting phase,²⁾⁻⁴⁾ the quarkyonic phase,⁵⁾ the inhomogeneous chiral condensed phase,⁶⁾ the quark ferromagnetic phase,⁷⁾ the color-ferromagnetic phase,⁸⁾ the spin polarized phase due to the axial vector interaction⁹⁾⁻¹²⁾ or due to the tensor interaction.¹³⁾⁻²³⁾

In order to investigate the phase structure in quark matter at finite baryon density, various effective models of QCD are used because in the region of large quark chemical potential, the numerical simulation by using the lattice QCD did not work until now. One of the effective models of QCD, the Nambu-Jona-Lasinio (NJL) model²⁴⁾ is widely used^{25), 26)} because it contains chiral symmetry, an important QCD symmetry. This model has been used to describe quark matter in the region with large quark chemical potential at low temperature.²⁷⁾ The extended NJL model,

which includes a tensor-type four-point interaction and/or the vector-pseudovector-type four-point interaction between quarks, is introduced to investigate the possible formation of a tensor condensate and/or pseudovector condensate, which may lead to the quark spin polarization.^{13)–18),21)–23),28)} If the quark spin polarization gives rise to spontaneous magnetization in quark matter, it may give origin to the strong magnetic field of compact stars such as neutron stars and magnetars.²⁹⁾

In this paper, we concentrate on the spin polarization due to the tensor condensate originated from the tensor interaction between quarks in an extended NJL model. In our previous paper in 19),20),30), the spin polarization due to the tensor condensate has been investigated widely in the case of the two-flavor NJL model. In this paper, we extend our previous work to the case of three-flavor NJL model. Previously, we have examined a possibility of conflict and/or coexistence of both the tensor condensate and the color-flavor locking condensate.¹⁷⁾ In three-flavor case, we have shown that two typical tensor condensates, which we name as F_3 ($= \langle \bar{\psi} \Sigma_3 \lambda_3 \psi \rangle$) and F_8 ($= \langle \bar{\psi} \Sigma_3 \lambda_8 \psi \rangle$), appear, where Σ_3 and λ_a are, respectively, the spin matrix with the third component (z -component) and the Gell-Mann matrices for $a = 1, \dots, 8$ or the identity matrix times $\sqrt{2/3}$ ($a = 0$). Also, a conjecture that $F_8 = F_3/\sqrt{3}$ is satisfied was given. However, in that paper, we have neglected both the flavor-symmetry breaking and the flavor mixing. If the flavor-symmetry is broken, the relation $F_8 = F_3/\sqrt{3}$ is not valid.

In a recent paper,³¹⁾ a spin polarization due to a tensor-type interaction in $2+1$ flavor NJL model has been investigated. The authors have introduced the two tensor condensates F_3 and F_8 correctly. However, they have assumed $F_8 = F_3/\sqrt{3}$ in most part of their analysis for numerical simplicity, while they have treated F_8 and F_3 independently only in the final part of their paper. As was previously mentioned, the approximate condition $F_8 = F_3/\sqrt{3}$ is valid in the chiral limit, i.e. if all the current quark masses are zero. Thus, we reanalyze the possible formation of the tensor condensates in 3-flavor cold quark matter at finite density. In three-flavor case, it is well known that the quark-flavor mixing occurs through the six-point interaction between quarks in the NJL model. This interaction is called the Kobayashi-Maskawa-'t Hooft interaction or the determinant interaction.^{32),33)} Thus, in this paper, we especially focus our attention on the effects of the flavor symmetry breaking and the flavor mixing through the Kobayashi-Maskawa-'t Hooft interaction on the tensor condensates.

This paper is organized as follows: In the next section, the mean field approximation for the NJL model with tensor-type four-point interaction between quarks is given. Then, both the quark and antiquark condensate, namely chiral condensate, and the two-type tensor condensates are introduced and further, the thermodynamic potential is evaluated at zero temperature with finite quark chemical potential. Both the condensates are treated self-consistently by means of the gap equations. In section 3, the solutions of the gap equations are numerically given and the behaviors of the tensor condensates and the dynamical quark masses related to the light quarks (u and d quarks) and the strange quark are investigated. The last section is devoted to a summary and concluding remarks.

§2. Mean field approximation for the Nambu-Jona-Lasinio model with tensor-type four-point interaction between quarks

Let us start from the three-flavor Nambu-Jona-Lasinio model with tensor-type^{14), 15)} four-point interactions between quarks. The Lagrangian density can be expressed as

$$\begin{aligned}
\mathcal{L} &= \mathcal{L}_0 + \mathcal{L}_m + \mathcal{L}_S + \mathcal{L}_T + \mathcal{L}_D , \\
\mathcal{L}_0 &= \bar{\psi} i \gamma^\mu \partial_\mu \psi , \\
\mathcal{L}_m &= -\bar{\psi} \vec{m}_0 \psi , \\
\mathcal{L}_S &= G_s \sum_{a=0}^8 [(\bar{\psi} \lambda_a \psi)^2 + (\bar{\psi} i \lambda_a \gamma_5 \psi)^2] , \\
\mathcal{L}_T &= -\frac{G_T}{4} \sum_{a=0}^8 [(\bar{\psi} \gamma^\mu \gamma^\nu \lambda_a \psi)(\bar{\psi} \gamma_\mu \gamma_\nu \lambda_a \psi) + (\bar{\psi} i \gamma_5 \gamma^\mu \gamma^\nu \lambda_a \psi)(\bar{\psi} i \gamma_5 \gamma_\mu \gamma_\nu \lambda_a \psi)] , \\
\mathcal{L}_D &= -G_D [\det \bar{\psi} (1 - \gamma_5) \psi + \det \bar{\psi} (1 + \gamma_5) \psi] , \tag{1}
\end{aligned}$$

where \vec{m}_0 represents a current quark mass matrix in flavor space as follows :

$$\vec{m}_0 = \text{diag} (m_u, m_d, m_s) . \tag{2}$$

Here, \mathcal{L}_T represents a four-point tensor interaction between quarks in the three-flavor case which preserves chiral symmetry. Also, \mathcal{L}_D represents so-called the Kobayashi-Maskawa-'t Hooft or the determinant interaction term which leads to the six-point interaction between quarks in the three-flavor case. In this paper, we introduce minus sign in \mathcal{L}_D in which we take $G_D > 0$ from the beginning.

Hereafter, we treat the above model within the mean field approximation and ignore non-diagonal components of the condensates in a flavor space. Therefore, terms in the summation over a are restricted to the diagonal entries with $a = 0, 3$ and 8 in \mathcal{L}_S :

$$\begin{aligned}
\sum_{a=0}^8 [(\bar{\psi} \lambda_a \Gamma \psi)^2] &\longrightarrow \sum_{a=0,3,8} [(\bar{\psi} \lambda_a \Gamma \psi)^2] \\
&= \frac{2}{3} [(\bar{u} \Gamma u + \bar{d} \Gamma d + \bar{s} \Gamma s)]^2 + [(\bar{u} \Gamma u - \bar{d} \Gamma d)]^2 \\
&\quad + \frac{1}{3} [(\bar{u} \Gamma u + \bar{d} \Gamma d - 2\bar{s} \Gamma s)]^2 \\
&= 2(\bar{u} \Gamma u)^2 + 2(\bar{d} \Gamma d)^2 + 2(\bar{s} \Gamma s)^2 . \tag{3}
\end{aligned}$$

Here, Γ means products of any gamma matrices or unit matrix. Also, in the determinant interaction term, \mathcal{L}_D , the same approximation is adopted, namely, the off-diagonal matrix elements in the flavor space are omitted:

$$\begin{aligned}
&\det \bar{\psi} (1 - \gamma_5) \psi + \det \bar{\psi} (1 + \gamma_5) \psi \\
&\longrightarrow \det \begin{pmatrix} \bar{u}(1 - \gamma_5)u & 0 & 0 \\ 0 & \bar{d}(1 - \gamma_5)d & 0 \\ 0 & 0 & \bar{s}(1 - \gamma_5)s \end{pmatrix}
\end{aligned}$$

$$\begin{aligned}
& + \det \begin{pmatrix} \bar{u}(1 + \gamma_5)u & 0 & 0 \\ 0 & \bar{d}(1 + \gamma_5)d & 0 \\ 0 & 0 & \bar{s}(1 + \gamma_5)s \end{pmatrix} \\
& = 2(\bar{u}u)(\bar{d}d)(\bar{s}s) \\
& \quad + 2(\bar{u}u)(\bar{d}\gamma_5 d)(\bar{s}\gamma_5 s) + 2(\bar{u}\gamma_5 u)(\bar{d}d)(\bar{s}\gamma_5 s) + 2(\bar{u}\gamma_5 u)(\bar{d}\gamma_5 d)(\bar{s}s) .
\end{aligned} \tag{4}$$

Secondly, in order to consider the spin polarization under the mean field approximation, the tensor condensate $\langle \bar{q}\gamma^1\gamma^2 q \rangle$ and $\langle \bar{q}\gamma^2\gamma^1 q \rangle$ are considered in \mathcal{L}_T because $\gamma^1\gamma^2 = i\Sigma_3$. Here,

$$\Sigma_3 = -i\gamma^1\gamma^2 = \begin{pmatrix} \sigma_3 & 0 \\ 0 & \sigma_3 \end{pmatrix} , \tag{5}$$

where σ_3 represents the third component of the Pauli matrix. Thus, we consider two tensor condensates under the mean field approximation as

$$\begin{aligned}
F_3 &= -G_T \langle \bar{\psi} \Sigma_3 \lambda_3 \psi \rangle , \\
F_8 &= -G_T \langle \bar{\psi} \Sigma_3 \lambda_8 \psi \rangle .
\end{aligned} \tag{6}$$

For each quark flavor, the tensor condensates are reexpressed as

$$\begin{aligned}
F_u &= F_3 + \frac{1}{\sqrt{3}}F_8 , \\
F_d &= -F_3 + \frac{1}{\sqrt{3}}F_8 , \\
F_s &= -\frac{2}{\sqrt{3}}F_8 .
\end{aligned} \tag{7}$$

Of course, the chiral condensates $\langle \bar{q}q \rangle$ should be taken into account. We introduce the dynamical quark masses \mathcal{M}_f without the determinant interaction term by using the chiral condensates as

$$\begin{aligned}
\mathcal{M}_u &= -4G_s \langle \bar{u}u \rangle , \\
\mathcal{M}_d &= -4G_s \langle \bar{d}d \rangle , \\
\mathcal{M}_s &= -4G_s \langle \bar{s}s \rangle .
\end{aligned} \tag{8}$$

These expressions are only valid if the mixing term is not considered.

Thus, under the mean field approximation, the Lagrangian density (1) reduces to

$$\begin{aligned}
\mathcal{L}_{MF} &= \bar{\psi}(i\gamma^\mu \partial_\mu - \vec{M}_q - \vec{F}\Sigma_3)\psi \\
&\quad - \sum_f \frac{\mathcal{M}_f^2}{8G_s} + \frac{F_3^2 + F_8^2}{2G_T} - \frac{G_D}{16G_s^3} \mathcal{M}_u \mathcal{M}_d \mathcal{M}_s ,
\end{aligned} \tag{9}$$

where $f = u, d$ or s and

$$\vec{M}_q = \text{diag.} \left(m_u + \mathcal{M}_u + \frac{G_D}{8G_s^2} \mathcal{M}_d \mathcal{M}_s , \right.$$

$$\begin{aligned}
& m_d + \mathcal{M}_d + \frac{G_D}{8G_s^2} \mathcal{M}_s \mathcal{M}_u , \\
& m_s + \mathcal{M}_s + \frac{G_D}{8G_s^2} \mathcal{M}_u \mathcal{M}_d \Big) \\
& = \text{diag.} (M_u, M_d, M_s) ,
\end{aligned} \tag{10}$$

where \vec{M}_q represents the constituent quark mass matrix with the flavor mixing due to the determinant interaction term.

Introducing the quark chemical potential μ in order to consider a quark matter at finite density, the Hamiltonian density can be obtained from the mean field Lagrangian density as

$$\begin{aligned}
\mathcal{H}_{MF} - \mu \mathcal{N} = & \bar{\psi} \left(-i\boldsymbol{\gamma} \cdot \boldsymbol{\nabla} + \vec{M}_q - \mu \gamma^0 + \vec{F} \Sigma_3 \right) \psi \\
& + \sum_f \frac{\mathcal{M}_f^2}{8G_s} + \frac{F_3^2 + F_8^2}{2G_T} + \frac{G_D}{16G_s^3} \mathcal{M}_u \mathcal{M}_d \mathcal{M}_s ,
\end{aligned} \tag{11}$$

where \mathcal{N} represents the quark number density, $\psi^\dagger \psi$.

Let us derive the effective potential or the thermodynamic potential at zero temperature. The Hamiltonian density (11) can be rewritten as

$$\mathcal{H}_{MF} - \mu \mathcal{N} = \psi^\dagger (h_T - \mu) \psi + \sum_f \frac{\mathcal{M}_f^2}{8G_s} + \frac{F_3^2 + F_8^2}{2G_T} + \frac{G_D}{16G_s^3} \mathcal{M}_u \mathcal{M}_d \mathcal{M}_s , \tag{12}$$

$$h_T = -i\gamma^0 \boldsymbol{\gamma} \cdot \boldsymbol{\nabla} + \gamma^0 \vec{M}_q + \vec{F} \Sigma_3. \tag{13}$$

In order to obtain the eigenvalues of the single-particle Hamiltonian h_T , namely the energy eigenvalues of single quark, it is necessary to diagonalize h_T , the eigenvalues of which can be obtained easily as

$$E_{p_1, p_2, p_3, \eta}^f = \sqrt{p_3^2 + \left(\sqrt{p_1^2 + p_2^2 + M_f^2} + \eta F_f \right)^2} , \tag{14}$$

where $\eta = \pm 1$.

Thus, we can easily evaluate the thermodynamic potential with the above single-particle energy eigenvalues. Then, the thermodynamic potential Φ can be expressed as

$$\begin{aligned}
\Phi = & \sum_{f, \alpha, \eta} \int \frac{dp_3}{2\pi} \int \frac{dp_1}{2\pi} \int \frac{dp_2}{2\pi} \left(E_{p_1, p_2, p_3, \eta}^f - \mu \right) \theta \left(\mu - E_{p_1, p_2, p_3, \eta}^f \right) \\
& - \sum_{f, \alpha, \eta} \int \frac{dp_z}{2\pi} \int \frac{dp_x}{2\pi} \int \frac{dp_y}{2\pi} E_{p_x, p_y, p_z, \eta}^f \\
& + \sum_f \frac{\mathcal{M}_f^2}{8G_s} + \frac{F_3^2 + F_8^2}{2G_T} + \frac{G_D}{16G_s^3} \mathcal{M}_u \mathcal{M}_d \mathcal{M}_s ,
\end{aligned} \tag{15}$$

where α represents the color degree which leads to numerical factor $N_c (= 3)$. Here, $\theta(x)$ represents the Heaviside step function. The first and second lines in (15) represent the positive-energy contribution of quarks and the vacuum contribution, respectively.

To determine the chiral condensates or the dynamical quark masses \mathcal{M}_f and the tensor condensates F_3 and F_8 , the gap equation is demanded as

$$\frac{\partial\Phi}{\partial\mathcal{M}_u} = \frac{\partial\Phi}{\partial\mathcal{M}_d} = \frac{\partial\Phi}{\partial\mathcal{M}_s} = \frac{\partial\Phi}{\partial F_3} = \frac{\partial\Phi}{\partial F_8} = 0. \quad (16)$$

§3. Numerical results

In this section, let us derive numerical results and give discussions about the effects of the flavor mixing.

First, we summarize the parameter sets with/without the determinant interaction which we call Model I/Model O, respectively. When we calculate the thermodynamic potential in (15), a regularization scheme is necessary because the vacuum contribution in the second line in (15) gives the divergent contribution. Here, we adopt the three-momentum cutoff scheme and introduce the three-momentum cutoff Λ . In Model O, which does not include the determinant interaction, the parameters are given so as to reproduce the pion decay constant and dynamical quark masses or pion mass and kaon mass. As for the tensor-type interaction, this interaction should be derived from a two-gluon exchange interaction in QCD.¹⁹⁾ However, since the NJL model cannot be derived from the QCD Lagrangian directly, we adopt G_T as a free parameter in this model. If we assume that the tensor-type interaction term is derived by the Fierz transformation of the scalar-type four-point interaction term, $G(\bar{\psi}\psi)^2$, in the NJL model, we can obtain the relationship $G_T = 2G_S$. On the other hand, the value of G_T can be determined by the vacuum properties of pion and ρ meson as in Ref.34). Since, in the following, we discuss the system at finite density, this treatment may not be adequate. Thus, we treat G_T as a free parameter. Similarly, in Model I in which the determinant interaction G_D is introduced, the model parameters are determined so as to reproduce the masses of eta and eta prime mesons adding to pion and kaon masses and the pion decay constant.²⁶⁾

3.1. Case of no flavor mixing (Model O)

Figure 1 shows two possible tensor condensation F_3 and F_8 as a function of the quark chemical potential μ without the determinant interaction (Model O), namely the flavor mixing does not occur. In this figure, as for F_8 , we plot $|F_8|$ because F_8 has

Table I. Parameter sets of 3-flavor NJL model without/with the determinant interaction (Model O/Model I).

	m_u [GeV]	m_d [GeV]	m_s [GeV]	G_s [GeV ⁻²]	G_T [GeV ⁻²]	G_D [GeV ⁻⁵]	Λ [GeV]
Model O	0.0055	0.0055	0.1375	5.5	$2G_s (=11.0)$	0	0.6314
Model I	0.0055	0.0055	0.1375	4.6	$2G_s (=9.2)$	$9.288/\Lambda^5$	0.6314

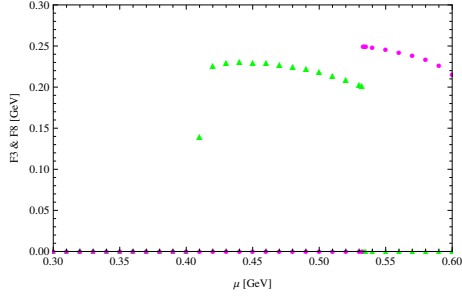


Fig. 1. Tensor condensates F_3 and $|F_8|$ are depicted as a function of the quark chemical potential μ . The triangle and circle represent F_3 and $|F_8|$, respectively.

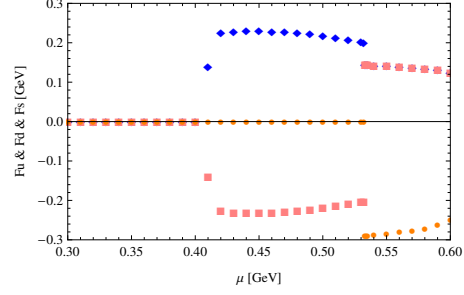


Fig. 2. Tensor condensates for each flavor are depicted as a function of the quark chemical potential μ . The diamond, square and circle represent F_u , F_d and F_s , respectively.

a negative sign. In this case, first, at $\mu \approx 0.41$ GeV, F_3 appears, which is represented by green triangle in Fig.1. At $\mu \approx 0.532$ GeV, F_3 suddenly disappears. Instead of F_3 , the condensate F_8 appears from $\mu \approx 0.532$ GeV and above it, which is represented by magenta circle in Fig.1. Thus, we conclude that two tensor condensates F_3 and F_8 does not coexist. Therefore, the relation $F_8 \approx F_3/\sqrt{3}$ should not be demanded. In Fig.2, the tensor condensates for each flavor, F_u (blue diamond), F_d (pink square) and F_s (orange circle) are depicted. As is seen in Fig.2, $F_u = -F_d$ is satisfied from $\mu \approx 0.41$ to 0.532 GeV in which only F_3 appears. Above $\mu \approx 0.532$ GeV, $F_u = F_d$ and $F_s = 2F_u$ are satisfied.

Figure 3 shows the constituent quark masses for $M_u (= M_d)$ (blue triangle) and M_s (violet circle), respectively. At $\mu \approx 0.34$ GeV, the light quark masses decrease. At $\mu \approx 0.53$ GeV, the strange quark mass decreases, but above $\mu \approx 0.53$ GeV, the strange quark mass is not so changed. If F_8 is set to 0, the strange quark mass decreases above $\mu \approx 0.55$ GeV. Thus, it is shown that the tensor condensate with respect to the strangeness, F_s leads to an almost constant strange quark mass and to the delay of the restoration of chiral symmetry for strangeness sector.

Figure 4 shows the contour plots of the thermodynamic potentials as (a) $\mu = 0.30$

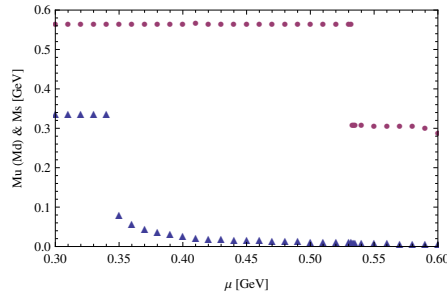


Fig. 3. Constituent quark masses $M_u = M_d$ (blue triangle) and M_s (violet circle) are depicted as a function of the quark chemical potential μ .

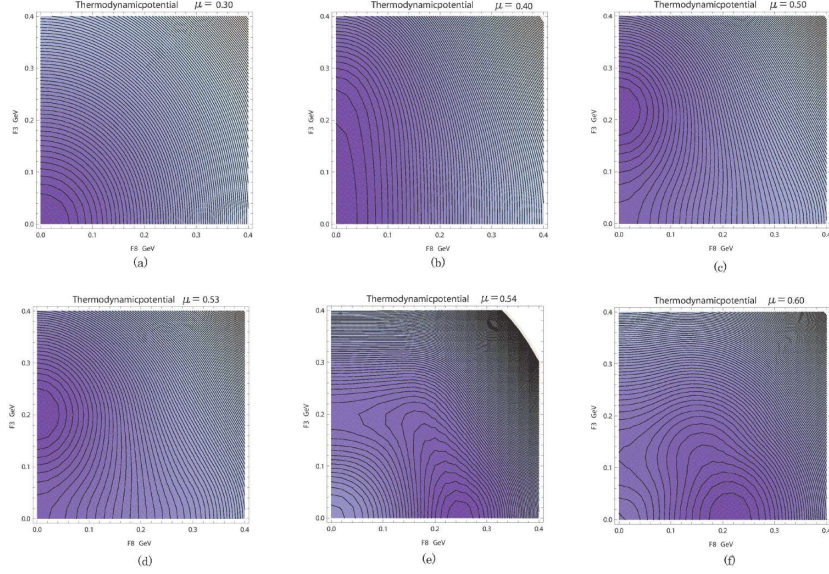


Fig. 4. Contour plots of the thermodynamic potentials are depicted as (a) $\mu = 0.30$ GeV, (b) $\mu = 0.40$ GeV, (c) $\mu = 0.50$ GeV, (d) $\mu = 0.53$ GeV, (e) $\mu = 0.54$ GeV and (f) $\mu = 0.60$ GeV. The horizontal and the vertical axes represent F_8 and F_3 , respectively.

GeV, (b) $\mu = 0.40$ GeV, (c) $\mu = 0.50$ GeV, (d) $\mu = 0.53$ GeV, (e) $\mu = 0.54$ GeV and (f) $\mu = 0.60$ GeV, respectively. The thermodynamic potential becomes lower as the color is darker in Fig.4. At $\mu = 0.30$ GeV, the tensor condensates does not appear, $F_3 = F_8 = 0$. Around $\mu = 0.40$ GeV, F_3 begins to appear. From Fig.4 (b), (c) and (d), the region from $\mu \approx 0.4$ to 0.53 GeV, the tensor condensate F_3 is non zero for the equilibrium configuration. However, at $\mu \approx 0.54$ GeV, F_3 disappears and F_8 appears.

3.2. Case of flavor mixing (Model I)

Next, we discuss the numerical results with flavor mixing due to the determinant interaction. This interaction leads to the important $U_A(1)$ -anomaly and the eta and eta prime mesons are well described.^{32), 33)}

Figure 5 shows two possible tensor condensation F_3 and F_8 as a function of the quark chemical potential μ with the determinant interaction (Model I) which leads to the flavor mixing. We also plot $|F_8|$ because F_8 has a negative sign. In this case, first, at $\mu \approx 0.48$, F_3 (green triangle) appears. At $\mu \approx 0.508$ GeV, F_8 suddenly appears and until $\mu \approx 0.52$ GeV, F_3 and F_8 coexist. Above $\mu \approx 0.52$ GeV, F_3 disappears and only F_8 remains. In Fig.6, the tensor condensates for each flavor, F_u (blue diamond), F_d (pink square) and F_s (orange circle) are depicted. Below $\mu \approx 0.508$ GeV, $F_u = -F_d$ satisfies. However, in the region of $\mu \approx 0.508 \sim 0.52$ GeV, both the relations $F_u = -F_d$ and $F_u = F_d$ are not valid. Above $\mu \approx 0.52$ GeV,

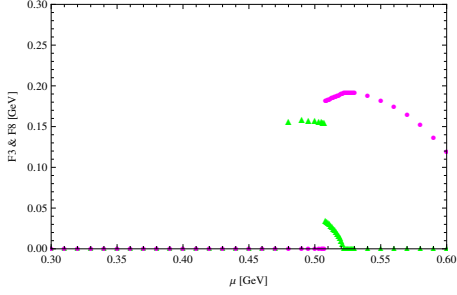


Fig. 5. Tensor condensates F_3 and F_8 are depicted as a function of the quark chemical potential μ . The triangle and circle represent F_3 and F_8 , respectively.

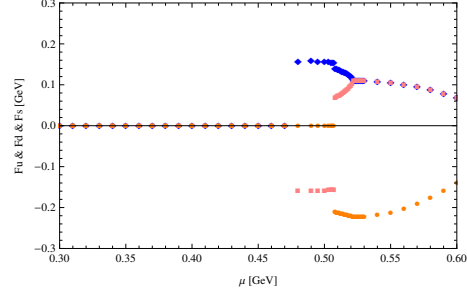


Fig. 6. Tensor condensates for each flavor are depicted as a function of the quark chemical potential μ . The diamond, square and circle represent F_u , F_d and F_s , respectively. Because $F_u = F_d$ is satisfied above $\mu \approx 0.52$ GeV, the symbols of diamond and square in this figure overlap.

$F_u = F_d$ and $F_s = 2F_u$ are satisfied now. This behavior is originated from the flavor mixing, while this behavior does not seen in the no flavor mixing case.

The fact that two tensor condensates coexist is shown by the absolute value of the thermodynamic potential. Figure 7 shows the value of the thermodynamic potential. The dashed line represents the value of the thermodynamic potential with F_3 only. The solid line represents the case with $F_3 \neq 0$ and $F_8 \neq 0$, namely, the value of the thermodynamic potential in which two tensor condensates coexist. Until $\mu \approx 0.507$ GeV, the thermodynamic potential with only $F_3 \neq 0$ is lower than the coexistence case of $F_3 \neq 0$ and $F_8 \neq 0$. However, at $\mu \approx 0.5075$ GeV, the situation is reversed. Above $\mu \approx 0.508$ GeV, the coexistence of F_3 and F_8 is preferred.

Figure 8 shows the constituent quark masses for $M_u (= M_d)$ (blue triangle) and M_s (violet circle), respectively. At $\mu \approx 0.34$ GeV, the light quark masses decrease. This behavior is the same as the result of no flavor mixing case. At $\mu \approx 0.508$ GeV,

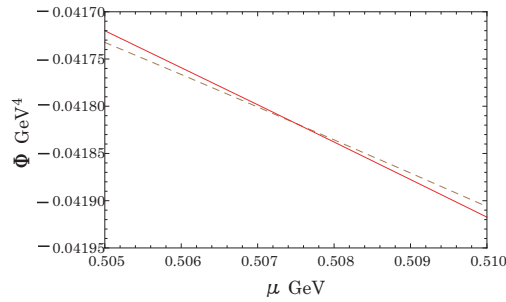


Fig. 7. The thermodynamic potential Φ is depicted as a function of the quark chemical potential μ . The dashed line represents the value of the thermodynamic potential with F_3 only. The solid line represents the case with $F_3 \neq 0$ and $F_8 \neq 0$, namely, the value of the thermodynamic potential in which two tensor condensates coexist.

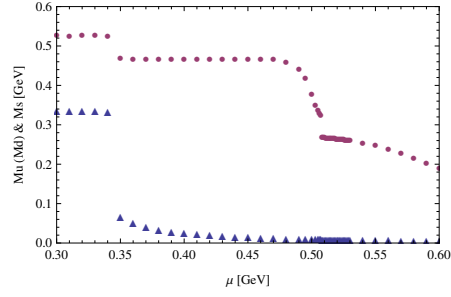


Fig. 8. Constituent quark masses $M_u = M_d$ (blue triangle) and M_s (violet circle) are depicted as a function of the quark chemical potential μ .

the strange quark mass has a small gap and the light quark mass has a fine structure. This is due to the flavor mixing through the constituent quark masses M_f . Above $\mu \approx 0.508$ GeV, the strange quark mass gradually decrease. This is originated from the appearance of the tensor condensate F_8 , namely F_s , as is seen in Fig.3. Thus, this behavior is not originated from the effect of the flavor mixing. .

Figure 9 shows the contour plots of the thermodynamic potentials as (a) $\mu = 0.30$ GeV, (b) $\mu = 0.48$ GeV, (c) $\mu = 0.50$ GeV, (d) $\mu = 0.51$ GeV, (e) $\mu = 0.51$ GeV same as (d) except for the scale and (f) $\mu = 0.60$ GeV, respectively. The thermodynamic

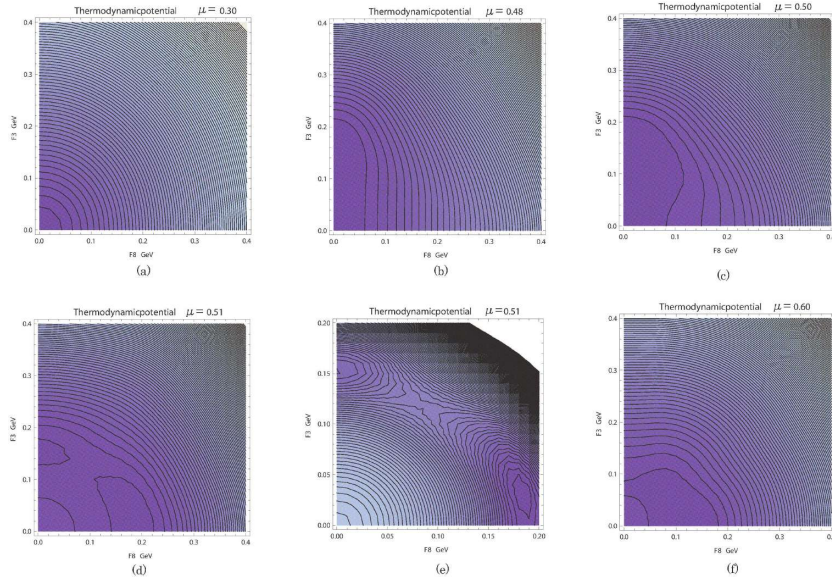


Fig. 9. Contour plots of the thermodynamic potentials are depicted as (a) $\mu = 0.30$ GeV, (b) $\mu = 0.40$ GeV, (c) $\mu = 0.50$ GeV, (d) $\mu = 0.53$ GeV, (e) $\mu = 0.54$ GeV and (f) $\mu = 0.60$ GeV. The horizontal and the vertical axes represent F_8 and F_3 , respectively.

potential decreases as the color becomes darker in Fig.9. At $\mu = 0.30$ GeV, the tensor condensates do not appear, $F_3 = F_8 = 0$. Around $\mu = 0.48$ GeV, F_3 begins to appear. At $\mu \approx 0.50$ GeV, F_3 has a finite value while $F_8 = 0$. However, at $\mu \approx 0.51$ GeV, F_8 begins to take a finite value adding to F_3 . The detailed behavior at $\mu = 0.51$ GeV is shown in Fig.9 (e). In (e), two local minima are seen. One is at the position with $F_3 \approx 0.15$ GeV and $F_8 = 0$ and the other is at $F_3 \approx 0.02$ GeV and $F_8 \approx 0.19$ GeV. As is indicated in Fig.7, the right local minimum with $F_3 \neq 0$ and $F_8 \neq 0$ is a true minimum of the thermodynamic potential. Thus, there exists a region where the two tensor condensates coexist due to the effect of the flavor mixing.

§4. Summary and concluding remarks

The possible formation of tensor condensates in three-flavor cold quark matter has been investigated taking the Nambu-Jona-Lasinio model with the tensor-type four-point interaction as an effective model of QCD. In the three flavor case, it is necessary to consider the $U_A(1)$ anomaly which is incorporated in the Kobayashi-Maskawa-'t Hooft interaction or so-called determinant interaction with six-point interaction between quarks. In our previous work,¹⁷⁾ the tensor condensates has been investigated against the color-flavor locked state which leads to a color superconducting phase. In that paper, we showed that two tensor condensates may appear which we denote by F_3 and F_8 . Besides, we have treated only the three-flavor system in the chiral limit, namely all current quark masses being zero. As a result, the two condensates were related with each other, namely $F_8 = F_3/\sqrt{3}$, when all the current quark masses are the same. In Ref.31), the tensor condensates has also been considered within the three-flavor NJL model with tensor interaction and the determinant interaction. However, almost all results have been obtained under the ansatz of $F_8 = F_3/\sqrt{3}$. In the present study, we did not consider this last approximation. Instead, we have estimated both tensor condensates independently within the three-flavor NJL model with tensor interaction. In both the cases of the flavor mixing due to the determinant interaction and no flavor mixing, we have reinvestigated the cold quark matter with the finite quark chemical potential. We have confirmed that the ansatz of $F_8 = F_3/\sqrt{3}$ is not valid except for the case of chiral limit.

Focusing on the determinant interaction in the three-flavor NJL model, which leads to the quark-flavor mixing, we have investigated the effect of flavor mixing on the two types of the tensor condensates and dynamical quark masses. As a result, the quantities related to the strange quark are affected by the determinant interaction, especially the behavior of the dynamical quark mass as a function of the quark chemical potential, while the quantities related to the light quarks are hardly affected. The tensor condensate related to the strange quark occurs at a rather small quark chemical potential compared with the case of no flavor mixing, namely, the case without the determinant interaction. The different behavior of the quark masses, which depend strongly on the presence of the determinant interaction, is the cause of this result. These behaviors are the same as the ones seen in the pseudovector condensates and the dynamical masses with pseudovector interaction and the flavor mixing.¹²⁾ Under the model parameters used in this paper, the tensor condensate

for light quarks and one for the strange quark coexist in a certain region of the quark chemical potential. On the other hand, if the flavor mixing is switched off, the coexistence region disappears. Thus, it is regarded as the effect of the flavor mixing.

The tensor condensates may lead to quark spin polarization. Therefore, to clarify the magnetic properties such as the spontaneous magnetization and magnetic susceptibility, it is interesting to investigate this problem in future studies. Further, the implication to the compact stars such as neutron stars and magnetars should be investigated by assuming the existence of the tensor condensates, related to the light quarks and the strange quark, while we have investigated the effect of the tensor condensate on the radius-mass relation of the hybrid quark star in the two-flavor case.³⁰⁾ This may be interesting future problem.

Acknowledgements

Three of the authors (A.K, M.M and Y.T.) would like to express their sincere thanks to Professor K. Iida and Dr. E. Nakano for their helpful comments.

References

- 1) K. Fukushima and T. Hatsuda, *Rep. Prog. Phys.* **74**, 014001 (2011).
- 2) M. Alford, K. Rajagopal and F. Wilczek, *Nucl. Phys. B* **537**, 443 (1999).
- 3) K. Iida and G. Baym, *Phys. Rev. D* **63**, 074018 (2001).
- 4) M. G. Alford, A. Schmitt, K. Rajagopal and T. Schafer, *Rev. Mod. Phys.* **80**, 1455 (2008) and references cited therein.
- 5) L. McLerran and R. D. Pisarski, *Nucl. Phys. A* **796**, 83 (2007).
- 6) E. Nakano and T. Tatsumi, *Phys. Rev. D* **71**, 114006 (2005).
- 7) T. Tatsumi, *Phys. Lett. B* **489**, 280 (2000).
- 8) A. Iwazaki, O. Morimatsu, T. Nishikawa and M. Ohtani, *Int. J. Mod. Phys. A* **22**, 721 (2007).
- 9) E. Nakano, T. Maruyama and T. Tatsumi, *Phys. Rev. D* **68**, 105001 (2003).
- 10) T. Tatsumi, T. Maruyama and E. Nakano, *Prog. Theor. Phys. Suppl.* No. 153, 190 (2004).
- 11) M. Morimoto, Y. Tsue, J. da Providência, C. Providência and M. Yamamura, *Int. J. Mod. Phys. E* **27**, 1850028 (2018).
- 12) M. Morimoto, Y. Tsue, J. da Providência, C. Providência and M. Yamamura, To appear in *Int. J. Mod. Phys. E* (2020).
- 13) H. Bohr, P. K. Panda, C. Providência and J. da Providência, *Braz. J. Phys.* **42**, 68 (2012).
- 14) H. Bohr, P. K. Panda, C. Providência and J. da Providência, *Int. J. Mod. Phys. E* **22**, 1350019 (2013).
- 15) Y. Tsue, J. da Providência, C. Providência and M. Yamamura, *Prog. Theor. Phys.* **128**, 507 (2012).
- 16) Y. Tsue, J. da Providência, C. Providência, M. Yamamura and H. Bohr, *Prog. Theor. Exp. Phys.* **2013**, Issue 10, 103D01 (2013).
- 17) Y. Tsue, J. da Providência, C. Providência, M. Yamamura and H. Bohr, *Prog. Theor. Exp. Phys.* **2015**, Issue 1, 013D02 (2015).
- 18) Y. Tsue, J. da Providência, C. Providência, M. Yamamura and H. Bohr, *Prog. Theor. Exp. Phys.* **2015**, Issue 10, 103D01 (2015).
- 19) H. Matsuoka, Y. Tsue, J. da Providência, C. Providência, M. Yamamura and H. Bohr, *Prog. Theor. Exp. Phys.* **2016**, Issue 5, 053D02 (2016).
- 20) H. Matsuoka, Y. Tsue, J. da Providência, C. Providência and M. Yamamura, *Phys. Rev. D* **95**, 054025 (2017).
- 21) E. J. Ferrer, V. de la Incera, I. Portillo and M. Quiroz, *Phys. Rev. D* **89**, 085034 (2014).
- 22) T. Maruyama and T. Tatsumi, *Phys. Rev. D* **96**, 096016 (2017).
- 23) T. Maruyama, E. Nakano, K. Yanase and N. Yoshinaga, *Phys. Rev. D* **97**, 114014 (2018).
- 24) Y. Nambu and G. Jona-Lasinio, *Phys. Rev.* **122**, 345 (1961), *Phys. Rev.* **124**, 246 (1961).

- 25) S. P. Klevansky, *Rev. Mod. Phys.* **64**, 649 (1992).
- 26) T. Hatsuda and T. Kunihiro, *Phys. Rep.* **247**, 221 (1994).
- 27) M. Buballa, *Phys. Rep.* **407**, 205 (2005).
- 28) S. Maedan, *Prog. Theor. Phys.* **118**, 729 (2007).
- 29) A. K. Harding and D. Lai, *Rept. Prog. Phys.* **69**, 2631 (2006).
- 30) H. Matsuoka, Y. Tsue, J. da Providência, C. Providência and M. Yamamura, *Phys. Rev. D* **98**, 074027 (2018).
- 31) A. Abhishek, A. Das, H. Mishra and R. K. Mohapatra, *Phys. Rev D* **100**, 114012 (2019).
- 32) M. Kobayashi and T. Maskawa, *Prog. Theor. Phys.* **44**, 1422 (1970).
- 33) G. 't Hooft, *Phys. Rev. D* **14**, 3432 (1976). [Erratum, *ibid. D* **18**, 2199 (1978).]
- 34) M. Jaminon, M. C. Ruvio and C. A. de Sousa, *Int. J. Mod. Phys. A* **17**, 4903 (2002).